Plant Physiology and Biochemistry 226 (2025) 110059

Contents lists available at ScienceDirect

Plant Physiology and Biochemistry

journal homepage: www.elsevier.com/locate/plaphy

Oryza sativa iron regulated transporter 1 (OsIRT1) and OsIRT2 are involved in ferrous iron uptake in rice

Deka Reine Judesse Soviguidi [a], Huaqian Ping [a,b], Bangzhen Pan [a,b], Rihua Lei [a,b], Gang Liang [a,b,*]

[a] Key Laboratory of Tropical Plant Resources and Sustainable Use, Chinese Academy of Sciences, Xishuangbanna Tropical Botanical Garden, Kunming, Yunnan, 650223, China
[b] The College of Life Sciences, University of Chinese Academy of Sciences, Beijing, China

ARTICLE INFO

Handling Editor: Dr K Kees Venema

Keywords:
Rice
Iron homeostasis
OsIRT1
OsIRT2
OsPRI1
OsPRI2

ABSTRACT

Iron (Fe) acquisition from soil is necessary for the normal growth and development of plants. *OsIRT1* and *OsIRT2* are induced by Fe deficiency; however, it remains unknown if they are required for Fe acquisition due to lack of their loss-of-function mutants. Here, we characterized the function of OsIRT1 and OsIRT2. We found that both OsIRT1 and OsIRT2 could rescue the deficiency symptoms of Arabidopsis *Atirt1* when they were driven by the CaMV35S promoter. The CRISPR-Cas9 technology was employed to generate various mutants, *Osirt1*, *Osirt2*, and *Osirt1/Osirt2*. Under hydroponic growth conditions with various Fe status, including Fe-free (-Fe), Fe(II), and Fe (III), no visible phenotypic differences were observed between mutants and wild type. Expression of the Strategy II genes was activated in the mutants under Fe-deficient conditions. Fe measurement showed that Fe concentrations were lower in mutants than in wild type under Fe(II) conditions, but not under -Fe and Fe(III) conditions. When grown in paddy field, the seed Fe concentration was lower in mutants than in wild type. Expression analysis indicated that the OsbHLH IVc member, OsPRI1, was required for the upregulation of *OsIRT1* and *OsIRT2* in response to Fe deficiency. Furthermore, OsPRI1 and OsPRI2 associate with and activate the promoters of *OsIRT1* and *OsIRT2*. This study characterizes the functions of OsIRT1 and OsIRT2 in the Fe(II) uptake, providing insights into the molecular mechanism of Fe homeostasis maintenance in rice.

1. Introduction

Iron (Fe) is an essential nutrient for plants, as it serves as a vital cofactor for a multitude of enzymes that participate in photosynthesis, chlorophyll biosynthesis, and respiration (Rai et al., 2021; Mahawar et al., 2023). However, the limited bioavailability of Fe, especially in alkaline soils, poses a major threat to plant growth and development. Plants growing under Fe-deficient conditions develop a chlorotic phenotype, shrunken leaves, and dwarf growth, leading to significant loss of crop yield (Gautam et al., 2021; Ning et al., 2023). In humans, Fe deficiency can cause severe anemia, particularly affecting young children and pregnant women, due to the reduced Fe content of staple food crops like cereals (Divte et al., 2021; Pasricha et al., 2021). Although rice (*Oryza sativa*) is one of the staple foods for more than half of the world's population, its Fe content is insufficient to meet human demand (Huang et al., 2020; Pradhan et al., 2020). Therefore, increasing Fe content of rice through biofortification is considered an effective strategy to combat widespread Fe deficiency.

Plants employ two different strategies to absorb Fe in a starved environment. Non-grass use the Fe uptake strategy I, which requires the reduction of ferric Fe [Fe(III)] to ferrous Fe [Fe(II)] prior to the transport of Fe(II) by IRT1 (Robinson et al., 1999; Vert et al., 2002). In contrast, grass plants use the strategy II, which involves the secretion of mugineic acids that chelate insoluble Fe(III) and facilitate its transport into the roots (Takagi, 1976; Takagi et al., 1984). As a special grass plant, rice also directly utilizes Fe(II) since it can grow in waterlogged fields, where most Fe elements exist as Fe(II) due to the low redox potential (Ishimaru et al., 2006). This dual ability enables rice plants to benefit from the advantages of each strategy, thus enhancing their chances of growth and survival in fluctuating Fe environments.

IRT1, a member of the zinc-regulated transporter/iron-regulated transporter-like proteins (ZIP) family, has been extensively studied in *Arabidopsis thaliana* for its pivotal role in Fe uptake (Soviguidi et al., 2025). Beyond its role in Fe transport, IRT1 also contributes to the

* Corresponding author. The College of Life Sciences, University of Chinese Academy of Sciences, Beijing, China.
E-mail address: lianggang@xtbg.ac.cn (G. Liang).

https://doi.org/10.1016/j.plaphy.2025.110059
Received 23 March 2025; Received in revised form 7 May 2025; Accepted 21 May 2025
Available online 22 May 2025

uptake of non Fe-metals such as zinc (Zn), cadmium (Cd), cobalt (Co), and manganese (Mn) (Korshunova et al., 1999; Rogers et al., 2000; Vert et al., 2002). Numerous studies have revealed the involvement of IRT1 in regulating Fe absorption in Arabidopsis (Eide et al., 1996; Vert et al., 2001, 2002; Connolly et al., 2002; Henriques et al., 2002; Varotto et al., 2002). In grass plants, HvIRT1 was required for Mn uptake but not Fe uptake although it has the ability to transport Fe in yeast, which raises the possibility that IRT1 may be not involved in Fe uptake in grass. In rice, both *OsIRT1* and *OsIRT2* are upregulated in response to Fe deficiency (Bughio et al., 2002; Bashir et al., 2014). The expression of *OsIRT1* and *OsIRT2* in yeast cells lacking the endogenous Fe(II) transporters *FET3* and *FET4* reversed the growth defect of the *fet3/fet4* double mutant (Ishimaru et al., 2006). Furthermore, transgenic rice plants overexpressing *OsIRT1* exhibited higher Fe accumulation than wild type plants when grown in Fe depleted media (Lee and An, 2009). However, it is still unknown if OsIRT1 and OsIRT2 are required for the Fe uptake in rice.

Plants perceive fluctuation of Fe status and modulate Fe signaling to maintain Fe homeostasis. HEMERYTHRIN MOTIF-CONTAINING PROTEIN 1 (OsHRZ1) and OsHRZ2 are the putative iron-binding sensors (Kobayashi et al., 2013), which interact with and may degrade OsbHLH IVc subgroup proteins including OsPRI1/OsbHLH60, OsPRI2/OsbHLH58, OsPRI3/OsbHLH59, and OsPRI4/OsbHLH057 (Zhang et al., 2017, 2020; Peng et al., 2022). OsPRI1, OsPRI2 and OsPRI3 activate the expression of *OsIRO2* and *OsIRO3*. OsIRO3, OsbHLH061 and OsbHLH062 belong to OsbHLH IVb subgroup, which recruit TOPLESS/TOPLESS-RELATED corepressors to negatively regulate iron homeostasis (Li et al., 2022; Wang et al., 2022; Li et al., 2025). FER-LIKE FE DEFICIENCY-INDUCED TRANSCRIPTION FACTOR(OsFIT/OsbHLH156) and OsIRO2 form a transcriptional complex to induce the expression of Strategy II genes, such as *OsNAS1*, *OsNAS2*, and *OsYL15* (Liang et al., 2020; Wang et al., 2020). ***OsIRT1*** expression **was reduced with the mutation of *OsFIT* and *OsIRO2*,** indicating that OsIRO2 and OsFIT positively regulate the expression of *OsIRT1* under Fe-deficient conditions (Liang et al., 2020). **In contrast, *OsIRT2* expression remained similar in** wild type **and *Osfit* mutants, suggesting that the upregulation of *OsIRT2* by Fe deficiency is likely independent of the OsFIT-OsIRO2 module** (Wang et al., 2020). Loss-of-function of OsPRI1 resulted in a significant downregulation of *OsIRT1* and *OsIRT2*, demonstrating that OsPRI1 is required for the induction of both genes (Zhang et al., 2017; Wang et al., 2022)**. However, it remains unclear if OsPRI1 directly regulates their expression under Fe deficiency.**

Due to lack of analysis of *OsIRT1* and *OsIRT2* loss-of-function mutants, there remains a significant gap in our understanding of their biological roles in rice. In the present study, we generated loss-of-function mutants of *OsIRT1* and *OsIRT2* and compared their Fe deficiency responses with wild type. We found that both OsIRT1 and OsIRT2 contributed to Fe(II) uptake, and the Strategy II pathway was activated with the mutation of *OsIRT1* and *OsIRT2*. Moreover, the *OsIRT1* and *OsIRT2* based Strategy I pathway is controlled by bHLH IVc proteins.

2. Results

2.1. OsIRT1 and OsIRT2 are able to rescue the Arabidopsis thaliana irt1 mutant

AtIRT1 is a necessary Fe transporter in Arabidopsis, since its mutation causes reduced Fe uptake and Fe deficiency symptoms (Vert et al., 2002). In contrast, plants with a mutation of *AtIRT2* were similar to wild type plants and overexpression of *AtIRT2* could not rescue *Atirt1* mutant (Varotto et al., 2002; Vert et al., 2009). When expressed transiently in Arabidopsis protoplasts, AtIRT1 was found on the plasma membrane, whereas AtIRT2 was labeled to the intracellular vesicles (Vert et al., 2009). However, both OsIRT1 and OsIRT2 were reported to localize to the plasma membrane when transiently expressed in the onion epidermal cells (Ishimaru et al., 2006). To further confirm their subcellular localization, Green fluorescent protein (GFP) was fused to the C-terminal of OsIRT1 and OsIRT2, and the corresponding recombinant OsIRT1-GFP and OsIRT2-GFP proteins were transiently expressed in tobacco (*Nicotiana benthamiana*) leaves under the control of the CaMV35S promoter. We observed that both OsIRT1 and OsIRT2 were localized to the plasma membrane (Fig. S1). Next, we asked whether OsIRT1 and OsIRT2 would be able to complement the Fe-deficient phenotype of the *Atirt1* mutant. In this regard, *OsIRT1* and *OsIRT2* under the control of the CaMV35S promoter were genetically introduced into *Atirt1-3* mutant plants by the deep floral immersion method. The complementary lines *Atirt1-3/OsIRT1-OE* and *Atirt1-3/OsIRT2-OE* were generated and the expression of *OsIRT1* and *OsIRT2* was confirmed by qRT-PCR (Fig. S2). When grown in soil, these lines developed better than *Atirt1-3* mutants that had chlorotic leaves (Fig. 1A). When grown on Fe-sufficient media, no visible differences were observed between complementation lines and *Atirt1-3*. However, on Fe-deficient media *Atirt1-3* displayed the typical Fe deficiency symptoms, and the complementation lines were similar to the wild type (Fig. 1B). These results indicated that overexpression of *OsIRT1* and *OsIRT2* is able to recover the Fe deficiency symptoms of the *Atirt1-3* mutant.

2.2. Loss-of-function of OsIRT1 and OsIRT2 causes reduced Fe(II) uptake

To investigate the biological functions of *OsIRT1* and *OsIRT2* in Fe deficiency response, the CRISPR/Cas9 editing system was used to generate their mutants. The target sites were designed and integrated into the editing vector, which were further introduced into the wild type via *Agrobacterium tumefaciens*-mediated transformation. *Osirt1*, *Osirt2*, and *Osirt1/Osirt2* mutant plants were generated and homozygous lines were identified by sequencing analysis. The *Osirt1-2* and *Osirt2-5* single mutants have a 1-bp insertion of G and C in their exon 1, respectively, which causes a frame-shift mutation (Fig. 2A and B). In the *Osirt1/Osirt2* double mutant, there is a 1-bp and 15-bp deletion in exon 1 of *OsIRT1* and *OsIRT2*, respectively, with the former causing a frame-shift mutation and the latter resulting in a deletion of 5 residues in the protein (Fig. 2C; Fig. S3).

To further clarify the functions of *OsIRT1* and *OsIRT2* in response to Fe deficiency, we performed hydroponic experiments. Wild type and mutant plants were exposed to nutrient solutions with different Fe contents: Fe free (-Fe), Fe(II) [0.05 mM EDTA-Fe(II)], and Fe(III) [0.05 mM EDTA-Fe(III)]. Hydroxylamine (0.1 mM) was added to the EDTA-Fe (II) solution to prevent Fe(II) oxidation. Regardless of the presence of Fe (II) or Fe(III), wild type and mutant plants developed similarly. Although the plants exhibited leaf chlorosis under Fe deficiency, no significant phenotypic differences were observed between wild type and mutants (Fig. 2D). Plant height and SPAD values also remained unchanged in both groups under all growth conditions (Fig. 2E and F).

Subsequently, we determined the Fe concentration in plants grown in hydroponic media. Under Fe-deficient and Fe(III) conditions, there were no difference in Fe concentration between mutants and wild type. In contrast, the Fe concentration in mutants was lower than that in wild type under Fe(II) conditions (Fig. 3A). We further assessed their growth in paddy field where both Fe(II) and Fe(III) were present. There were no differences in plant weight and grain yield. Although *Osirt1-2*, *Osirt2-5*, and *Osirt1/Osirt2* mutants did not exhibit obvious morphological changes, the Fe concentrations in their seeds were significantly reduced compared with the wild type (Fig. 3B). Taken together, these data suggest that *OsIRT1* and *OsIRT2* are required for Fe(II) uptake when Fe(II) is present.

2.3. Strategy II genes are increased in mutants

It was reported that the Strategy I pathway was activated when Strategy II pathway was blocked in the *naat1* mutant (Cheng et al., 2007). This implies that rice integrates both strategies to the

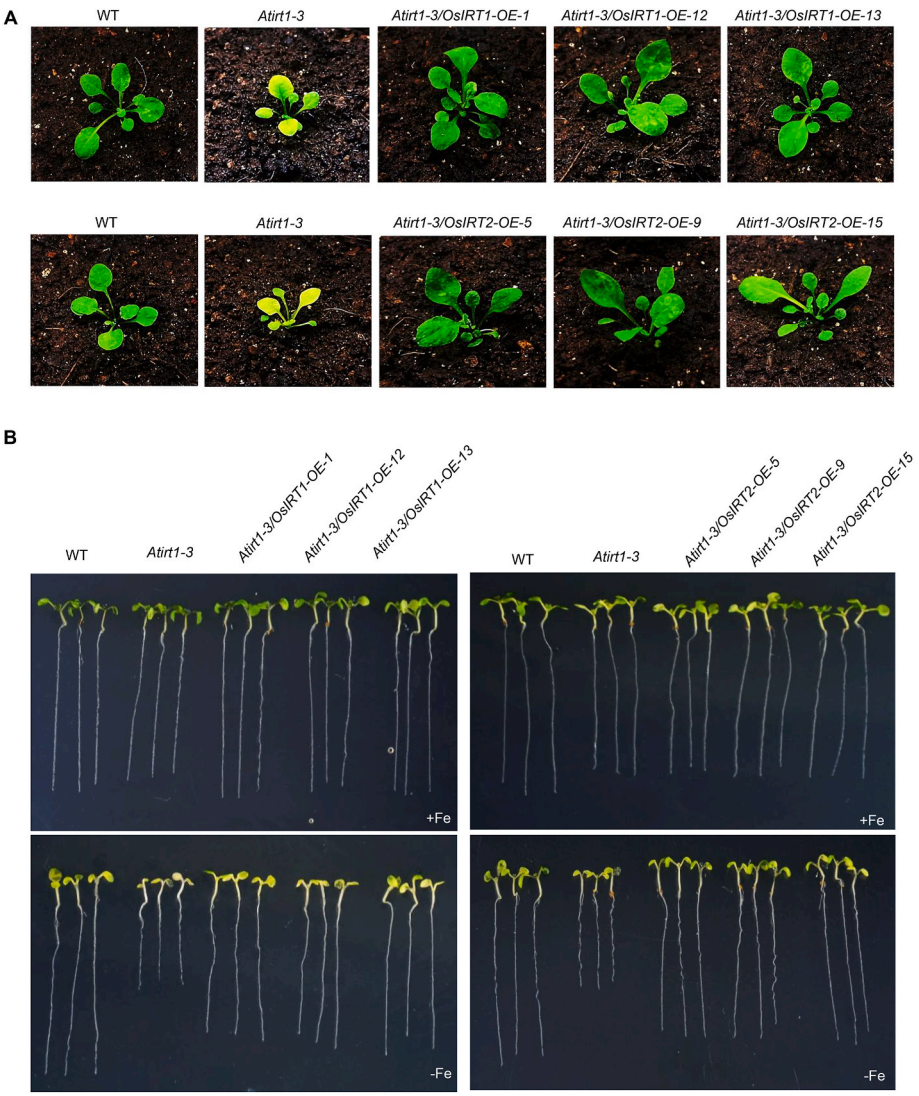

Fig. 1. Complementation of *Atirt1-3* (A)Phenotypes of plants. Three-week-old plants grown in soil are shown. (B)Phenotypes of seedlings. One-week-old seedlings grown on Fe-sufficient and Fe-deficient media.

maintenance of Fe homeostasis. Given that the Strategy I pathway was compromised in the mutants, we wanted to know if the Strategy II pathway was activated. To test this, we analyzed the expression of several Strategy II genes, such as *OsIRO2*, *OsNAS1*, *OsNAS2*, and *OsYSL15*, which have been shown to be upregulated under Fe-deficient conditions (Ishimaru et al., 2008). We found that under Fe-free conditions, the expression of *OsIRO2*, *OsNAS1*, *OsNAS2*, and *OsYSL15* was considerably enhanced in all mutants compared with wild type plants (Fig. 4A–D). Under Fe(II) conditions, *OsNAS1*, *OsNAS2*, and *OsYSL15* were upregulated in *Osirt2-5* and *Osirt1/Osirt2*. Under Fe(III) conditions, *OsIRO2* was increased in *Osirt1-2* and *OsNAS1* was increased in all mutants. These data suggest that the Strategy II pathway is activated, especially under Fe-deficient conditions, when the Strategy I pathway is disrupted.

2.4. *OsPRI1 and OsPRI2 directly activate the expression of OsIRT1 and OsIRT2*

Both *OsIRT1* and *OsIRT2* are induced considerably in response to Fe deficiency (Bughio et al., 2002; Bashir et al., 2014). Under Fe-deficient conditions, the expression of *OsIRT1* is slightly lower in *Osiro2* and *Osfit* than in wild type, whereas that of *OsIRT2* is higher in *Osiro2* and *Osfit* than in wild type (Liang et al., 2020). It implies that there are other transcription factors that activate the expression of *OsIRT1* and *OsIRT2* under Fe-deficient conditions. In addition to OsIRO2 and OsFIT, OsbHLH IVc subgroup are positive regulators of the Fe deficiency responses in rice. To investigate if OsbHLH IVc proteins are involved in the upregulation of *OsIRT1* and *OsIRT2*, we determined their expression in the four mutants of OsbHLH IVc members. Under Fe-deficient conditions, the expression of *OsIRT1* and *OsIRT2* was dramatically downregulated in the *Ospri1* (Fig. 5A and B). These results suggest that OsPRI1 positively regulates the expression of *OsIRT1* and *OsIRT2*.

Generally, bHLH family transcription factors specifically bind to E-box motif (CANNTG) or G-box (CACGTG, ACGTG, or CACGT) within their target DNA (Liu et al., 2015). Both E-box and G-box were found in the promoters of *OsIRT1* and *OsIRT2* (Fig. S4A). To determine whether OsbHLH IVc proteins bind to these G-boxes, yeast one-hybrid (Y1H) assays were performed with two representative OsbHLH IVc members, OsPRI1 and OsPRI2. OsPRI1 and OsPRI2 were fused to the pGAD vector as prey, while the *OsIRT1* and *OsIRT2* promoters were fused to the pAbAi vector as bait. Cells co-transformed with bait and prey were grown on SD/−Leu and SD/−Leu/AbA-resistant media. All combinations were able to grow normally on the SD/−Leu media. However, the various OsPRI/ProOsIRT combinations grew better than the control combinations (Fig. 6A and B). To further verify these results, EMSA was performed. The full length of *OsPRI1* and *OsPRI2* were fused with

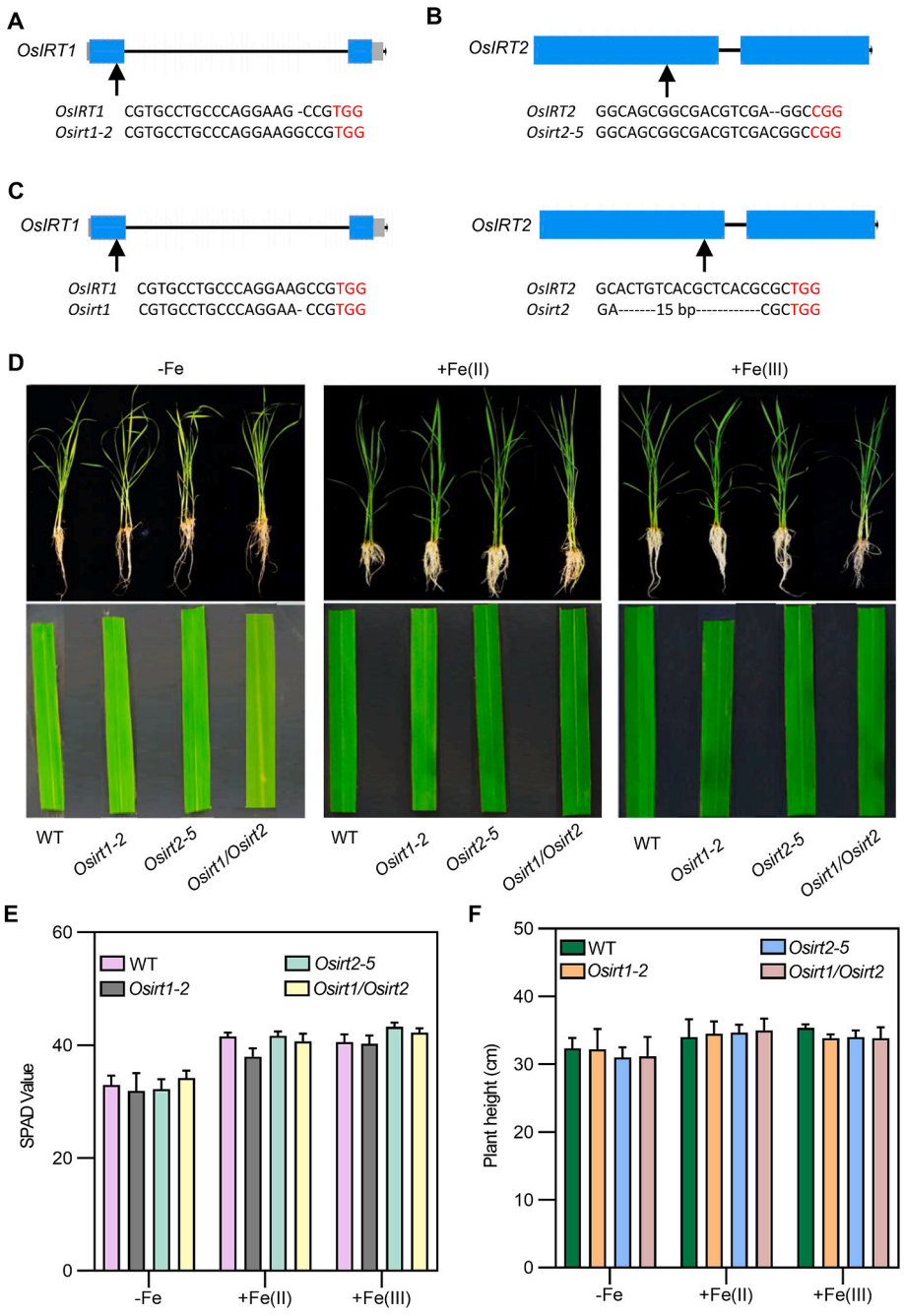

Fig. 2. Identification of various mutants. (A)Genotypes of *Osirt1-2*. (B)Genotypes of *Osirt2-5*. (C)Genotypes of *Osirt1/Osirt2*. (A–C) The arrows indicate the positions of target sequences. (D) Phenotypes of plants grown in different Fe solutions. Three-week-old plants are shown. The third leaves of seedlings are shown. Fe free (-Fe), Fe(II) [0.05 mM EDTA-Fe(II)], and Fe(III) [0.05 mM EDTA-Fe(III)]. (E) SPAD value. The third leaves were measured. (F) Plant height.

glutathione (GST), and the recombinant GST-OsPRI1 and GST-OsPRI2 proteins were expressed and purified from *Escherichia coli* cells. SDS-PAGE analysis was further performed to confirm protein integrity (Fig. S4B). When GST-OsPRI1 and GST-OsPRI2 were incubated with the biotin-labeled *OsIRT1* and *OsIRT2* probes, prominent protein-DNA complexes were detected. The binding capacity was inhibited by the addition of increasing amounts of unlabeled probe (Cold-Probe), but not mutated probe (Cold-mProbe) (Fig. 6C and D). These data suggest that OsPRI1 and OsPRI2 directly bind to the promoters of *OsIRT1* and *OsIRT2*.

Subsequently, transient expression assays were performed in tobacco leaves. The reporter plasmids with a fused nuclear localization signal GFP (*ProOsIRT1:nGFP* and *ProOsIRT2:nGFP)* were driven by the 1 kb DNA region upstream the translation start site of *OsIRT1* and *OsIRT2*. For effector plasmids, MYC-tagged OsPRI1 (MYC-OsPRI1) and mCherry-tagged OsPRI2 (mCherry-OsPRI2) were driven by the 35S promoter, respectively (Fig. 7A). *Pro35S:MYC* and Pro35S:mCherry vectors were used as negative effector controls. Each reporter was co-expressed with each of the effectors, respectively. The expression level of GFP was examined. The results indicated that OsPRI1 and OsPRI2 significantly increased the expression of GFP compared with the controls (Fig. 7B–E). Taken together, these results suggest that OsPRI1 and OsPRI2 directly bind to and activate the promoters of *OsIRT1* and *OsIRT2*.

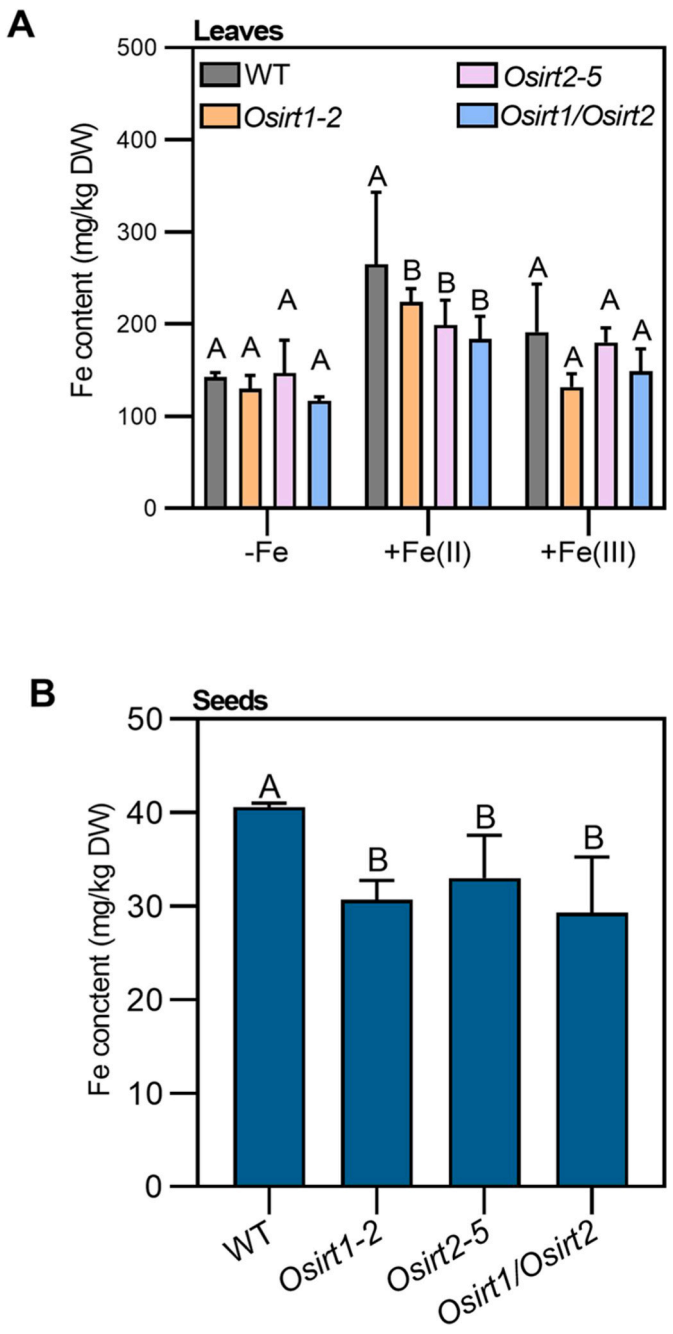

Fig. 3. Fe concentration in leaves and seeds. (A) Fe concentration in leaves. Plants were grown in different Fe solutions: Fe free (-Fe), Fe(II) [0.05 mM EDTA-Fe(II)], and Fe(III) [0.05 mM EDTA-Fe(III)]. One-month-old leaves were harvested for Fe quantification. (B) Fe concentration in seeds. Seeds were harvested from plants grown in paddy field. (A) and (B) Data represent means ± SD of three biological replicates ($n = 3$). Different letters above each bar indicate statistically significant differences as determined by one-way ANOVA followed by Tukey's multiple comparison test ($P < 0.05$).

3. Discussion

Higher plants employ two different strategies to absorb Fe from soil. Non-graminaceous plants use the reduction-based Strategy I and graminaceous plants utilize the chelation-based Strategy II. As a special graminaceous species, rice employs Strategy II and partial Strategy I to acquire Fe due to the abundant Fe(II) in the paddy field. OsIRT1 and OsIRT2 are considered two key components of the Strategy I Fe uptake system in rice; however, the functional roles of these two genes have not been comprehensively characterized. In this study, we provide evidence that OsIRT1 and OsIRT2 are involved in Fe(II) uptake in rice.

OsIRT1 and OsIRT2 are homologs of Arabidopsis AtIRT1 and AtIRT2, respectively. Although AtIRT1 and AtIRT2 have similar amino acid sequences, they play different roles in Fe uptake. While AtIRT1 is localized in plasma membrane (Vert et al., 2002), AtIRT2 is in the intracellular vesicles and can not rescue the Fe-deficient phenotypes caused by AtIRT1 loss-of-function (Vert et al., 2009). AtIRT1 is responsible for Fe uptake from soil to roots as well as Fe translocation from root to shoot, whereas AtIRT2 might be involved in Fe compartmentalization in cells (Vert et al., 2002, 2009). A previous report revealed no significant differences between wild type and *Atirt2* mutant plants, suggesting that AtIRT2 is not a key gene of the Strategy I system in Arabidopsis (Varotto et al., 2002). Unlike AtIRT2, OsIRT2 is a plasma membrane protein (Ishimaru et al., 2006). In this study, we found that both OsIRT1 and OsIRT2 were able to complement the Fe deficiency phenotypes of *Atirt1* mutant (Fig. 1A and B), probably due to their abilities in plasma membrane localization.

We observed no visible phenotype differences among *Osirt1*, *Osirt2*, *OsIRT1/Osirt2*, and wild type regardless of the Fe status (Fig. 2B and C). Thus, loss-of-function of *OsIRT1* or *OsIRT2* does not significantly enhance the Fe deficiency symptoms of plants grown under Fe-deficient conditions. However, the Fe concentration in leaves and seeds was lower in mutants than in wild type when Fe(II) is available in the rhizosphere (Fig. 3A and B), suggesting that OsIRT1 and OsIRT2 are required for Fe (II) uptake in rice. We noted that the Fe concentration in the *Osirt1/Osirt2* double mutant was not lower than that in the single mutants. In fact, there was a deletion of 5 residues in the OsIRT2 protein in the double mutant. The 5 residues contains three histidine (H) residues in the H-rich region of the cytosolic region in OsIRT2 (Fig. S3). It has been confirmed that the H residues in the cytosolic region of AtIRT1 are not required for Fe transport, but for sensing non-Fe metals (Dubeaux et al., 2018). This may explain why the double mutant acted like the *Osirt1* mutant regarding the Fe transport. On the other hand, there are other metal transporters which can take up Fe(II) in rice, such as NRAMP1 (Ishimaru et al., 2012). This may explain why mutation of *OsIRT1* or *OsIRT2* did not change the Fe deficiency symptoms of plants under Fe-deficient conditions. Further investigation with high order of mutants will establish contribution of the Strategy I to Fe homeostasis in rice.

This combined Strategy (Strategy II and partial Strategy I) is not specific to *O. sativa*. The orthologs of Strategy I genes, *IRT1*, *IRT2*, and *NRAMP1*, were also identified in nine species from the *Oryza genus*, maize and sorghum, and their responses to Fe deficiency are conserved in species of the *Oryza genus* closely related to domesticated rice, but not in maize or sorghum (Wairich et al., 2019). Thus, the adaptation to Fe (II) acquisition via IRT1 in flooded soils precedes *O. sativa* domestication. It is notable that HvIRT1 was characterized to mediate Mn uptake, but not Fe uptake, in barley (Long et al., 2018), although it is able to transport Fe in yeast and also induced by Fe deficiency in barley (Pedas et al., 2008). It is likely that the *Oryza genus* plants in Poaceae maintain this Fe(II) acquisition strategy. Rice plants accumulated more Fe in leaves under Fe(II) conditions than under Fe(III) conditions (Fig. 5AB), suggesting that Fe(II) uptake is more efficient than Fe(III) uptake. It may explain why rice plants possess Strategy I.

The Fe concentration in leaves and seeds decreased in mutants, which may be caused by the reduced root Fe(II) uptake. AtIRT1 was reported to mediate Fe transport from roots to shoots in Arabidopsis (Vert et al., 2002). Unlike *AtIRT1* that is specifically expressed in roots, *OsIRT1* is expressed both in roots and shoots, and its expression levels are higher in shoots than in roots under Fe-sufficient conditions. In response to Fe deficiency, *OsIRT1* is also induced in shoots. Thus, OsIRT1 might contribute to Fe translocation from roots to shoot as well as within shoots.

An earlier study showed that knockout of the Strategy II gene *NAAT1* affects the growth and development of *naat1* mutants under Fe(III)-supply conditions. Moreover, the expression of *OsIRT1* and *OsIRT2*

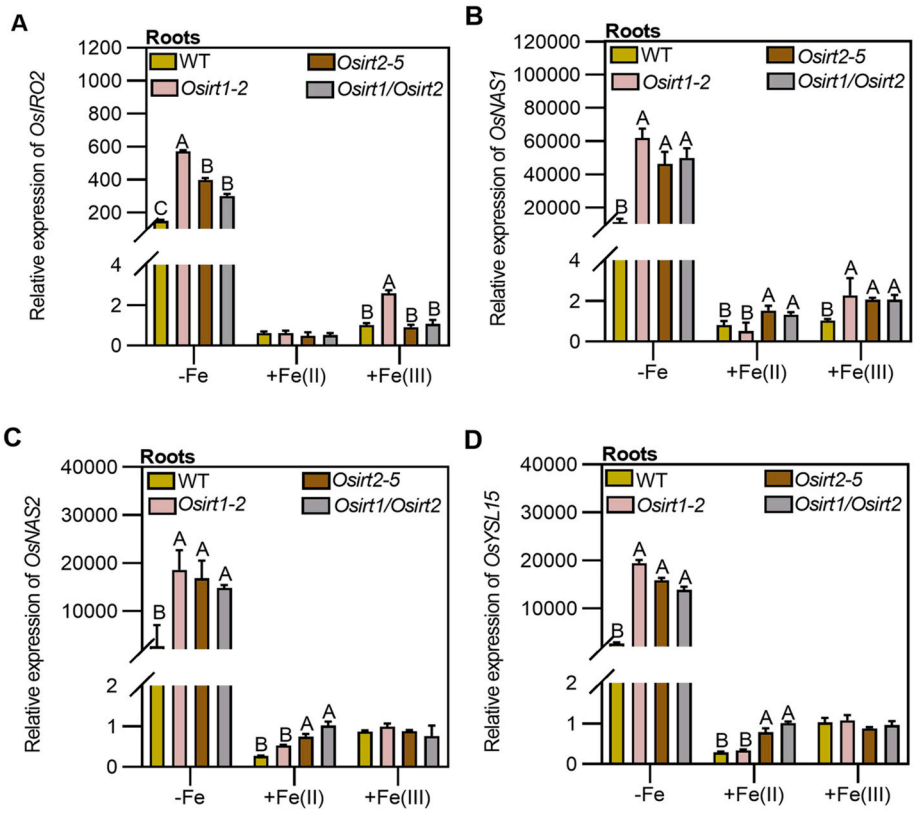

Fig. 4. Expression of Fe deficiency-inducible genes (A)Expression of *OsIRO2* (B)Expression of *OsNAS1* (C) Expression of *OsNAS2* (D)Expression of *OsYSL15* (A–D) One-week-old seedlings grown in Fe-sufficient media were shifted to various Fe solutions for 7 days. Fe free (-Fe), Fe(II) [0.05 mM EDTA-Fe(II)], and Fe(III) [0.05 mM EDTA-Fe(III)]. Data represent means ± SD of three biological replicates ($n = 3$). Different letters above each bar indicate statistically significant differences as determined by one-way ANOVA followed by Tukey's multiple comparison test ($P < 0.05$).

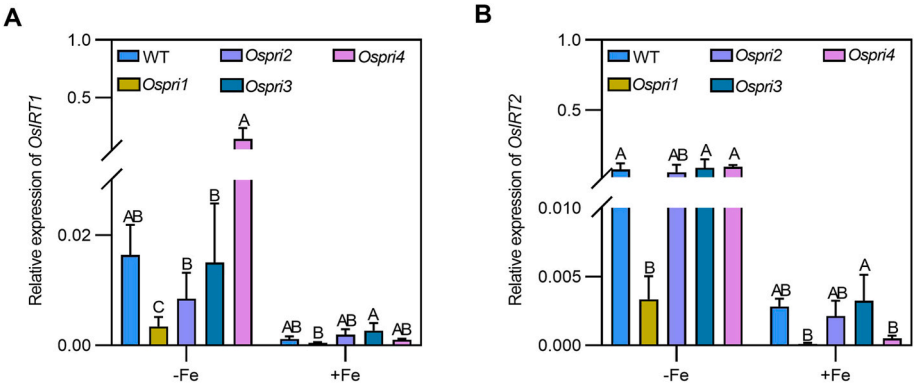

Fig. 5. Expression of *OsIRT1* and *OsIRT2* in the OsbHLH IVc mutants. (A)Expression of *OsIRT1*. (B)Expression of *OsIRT2*. One-week-old seedlings grown in Fe-sufficient media were shifted to Fe-sufficient or Fe-deficient media for 7 days. RNA was extracted from roots. Data represent means ± SD of three biological replicates ($n = 3$). Different letters above each bar indicate statistically significant differences as determined by one-way ANOVA followed by Tukey's multiple comparison test ($P < 0.05$).

was significantly upregulated in *naat1* mutants than in wild type plants when Fe(III) or Fe(II) was supplied as the sole Fe source. Additionally, under Fe(II) treatment, *naat1* mutants grew normally and accumulated significantly higher amounts of Fe in leaves and roots than wild type plants. These results suggest that the disruption of the Strategy II results in the activation of Strategy I in rice (Cheng et al., 2007). We found that the Strategy II genes *OsIRO2*, *OsNAS1*, *OsNAS2*, and *OsYSL15* were upregulated in all mutants under Fe-deficient conditions (Fig. 4A–D), implying that the disruption of Strategy I causes the activation of the Strategy II in rice. Since both strategies are required for Fe uptake and promoted by Fe deficiency, disruption of one strategy reduces Fe uptake and then leads to Fe deficiency, which in turn promotes the expression of the other Strategy genes. A similar phenomenon was observed in Arabidopsis that Fe deficiency inducible genes are constitutively activated in the *Atirt1* mutants with reduced Fe uptake (Wang et al., 2007).

Rice and Arabidopsis share remarkably similar Fe signaling pathways, although they possess different Fe uptake strategies (Liang, 2022). In Arabidopsis, the AtFIT-AtbHLH Ib complex controls the Strategy I Fe uptake system (Yuan et al., 2008). In rice, OsFIT interacts with OsIRO2 to positively regulate the Strategy II Fe uptake system. Except for *OsIRT1* that is slightly decreased in *Osfit* mutants, *OsIRT2* are not affected (Liang et al., 2020). Our results showed that the expression of both *OsIRT1* and

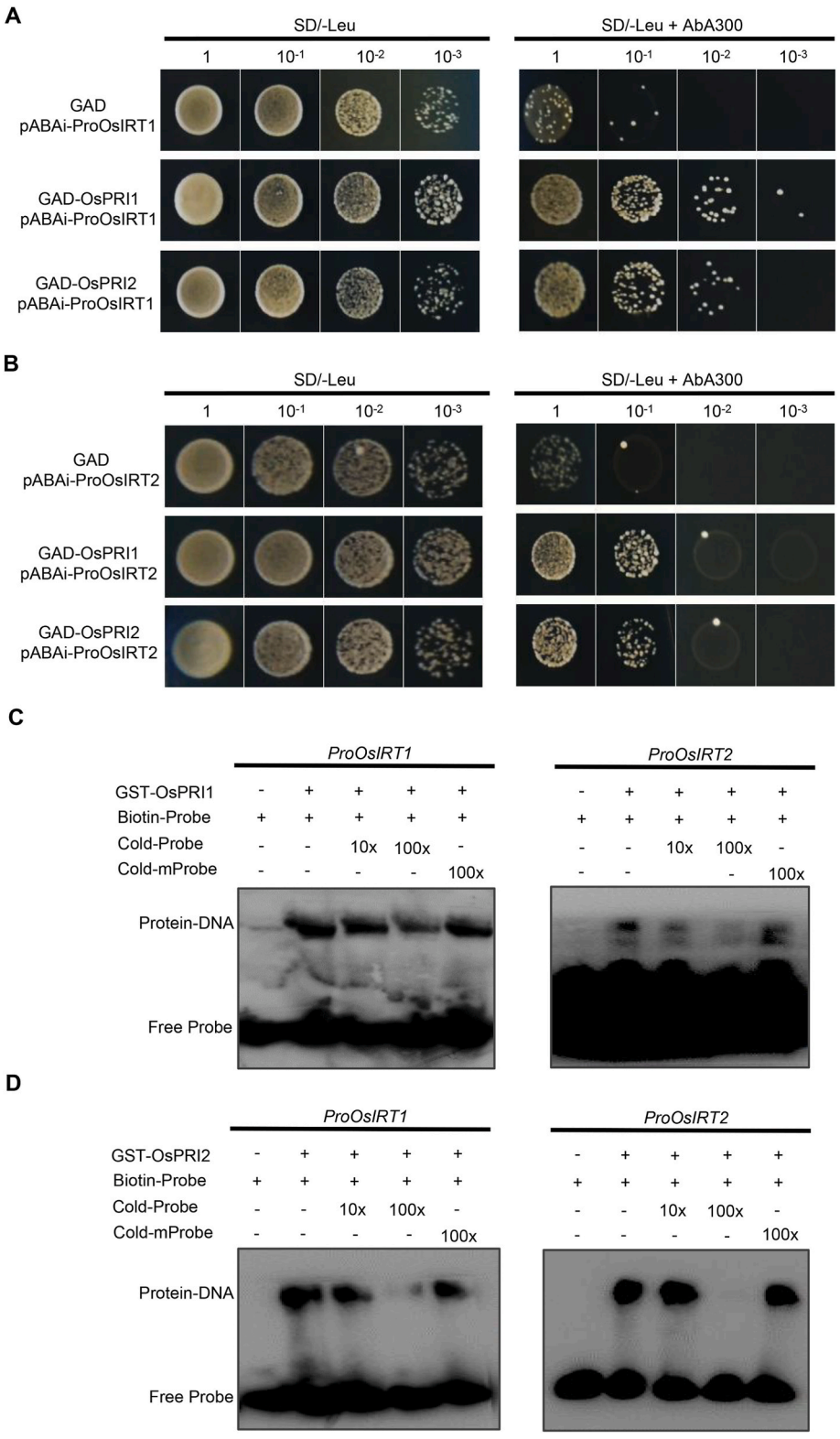

Fig. 6. OsPRI1 and OsPR2 bind to the promoters of OsIRT1 and OsIRT2. (A) Y1H assays showing that OsPRI1 and OsPRI2 bind to the promoter of *OsIRT1*. (B) Y1H assays showing that OsPRI1 and OsPRI2 bind to the promoter of *OsIRT2*. (C) EMSA showing that OsPRI1 binds to the promoters of OsIRT1 and OsIRT2. (D) EMSA showing that OsPRI2 binds to the promoters of OsIRT1 and OsIRT2.
and (D) Biotin-Probe (biotin-labeled probe), Cold-Probe (unlabeled probe), Cold-mProbe (unlabeled probe with mutated G-box).

OsIRT2 was decreased in the *Ospri1* mutants (Fig. 5A and B). In Arabidopsis, the four bHLH IVc members have strong functional redundancy (Li et al., 2016; Liang et al., 2017). Therefore, it is possible that the other three members also positively regulate *OsIRT1* and *OsIRT2*. Moreover, we further confirmed that OsPRI1 and OsPRI2 could directly bind to and activate the promoters of *OsIRT1* and *OsIRT2* (Fig. 6; Fig. 7). Finally, we draw a conclusion that OsbHLH IVc, at least OsPRI1, controls both Strategy I and Strategy II in rice.

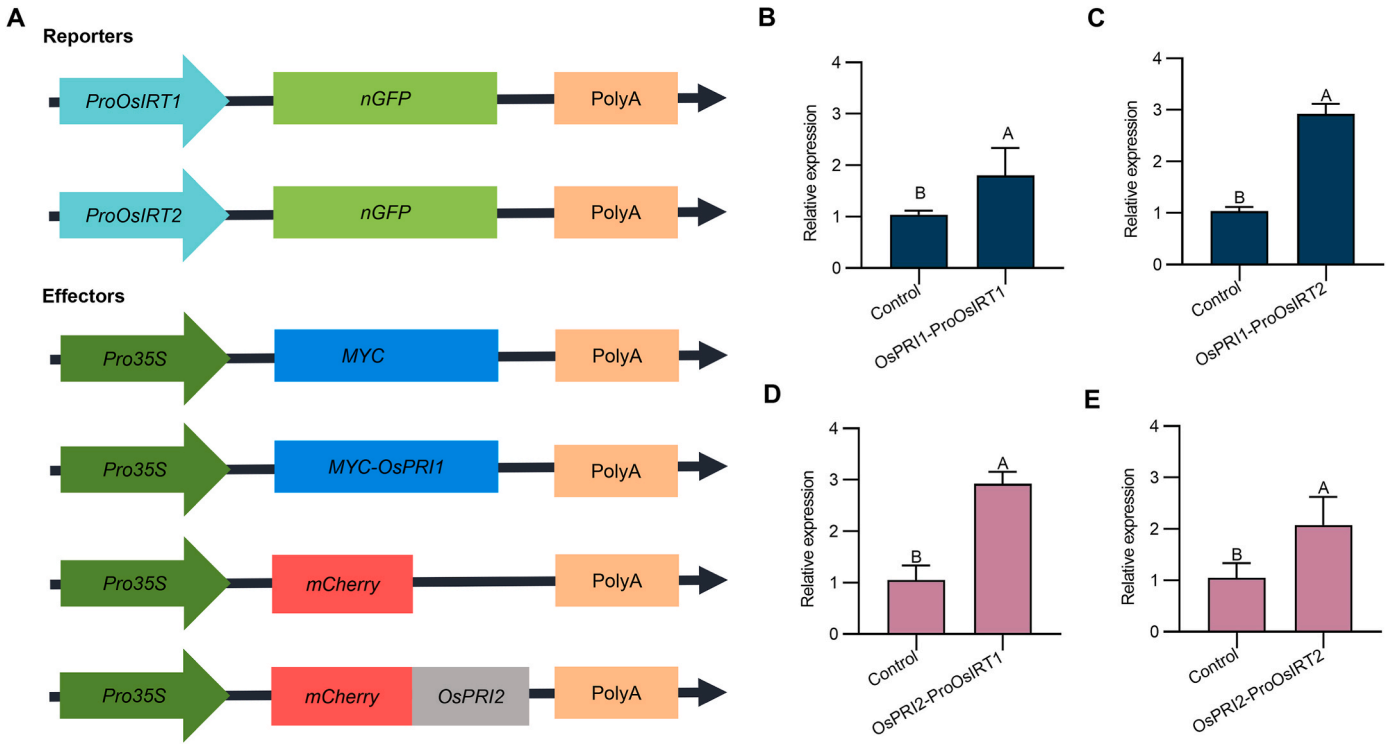

Fig. 7. OsPRI1 and OsPRI2 activate the promoters of *OsIRT1* and *OsIRT2*. (A) Schematic representation of the effector and reporter constructs used for transient expression assays. (B) OsPRI1 activates the promoter of *OsIRT1*. (C) OsPRI1 activates the promoter of *OsIRT2*. (D) OsPRI2 activates the promoter of *OsIRT1*. (E) OsPRI2 activates the promoter of *OsIRT2*. (B–E) GFP transcript abundance in infiltrated tobacco leaves. The tobacco leaves were harvested 48 h after infiltration for RNA extraction and qRT-PCR. GFP abundance was normalized to that of NPTII. Each bar represents the mean ± SD of three biological replicates ($n = 3$). Different letters above each bar indicate statistically significant differences as determined by one-way ANOVA followed by Tukey's multiple comparison test ($P < 0.05$).

4. Materials and methods

4.1. Plant materials and growth conditions

Oryza sativa L. cv. Nipponbare was used in this study. Rice seeds were germinated for 7 days and then transferred to hydroponic solutions containing half-strength Murashige and Skoog (MS) medium (pH 5.6–5.8) with 0.05 mM EDTA-Fe(II) or 0.05 mM EDTA-Fe(III) (+Fe), or without Fe (-Fe). Hydroxylamine (0.1 mM) was added to the EDTA-Fe (II) solution to prevent Fe(II) oxidation. The nutrient solution was changed every 3 days. Plants were grown in a growth chamber with a photoperiod of 14 h light at 25 °C and 10 h dark at 20 °C in the greenhouse.

4.2. Generation of transgenic plants

The CRISPR/Cas9 editing method described by Liang et al. (2016) was used to generate mutant plants. Briefly, two guide RNAs were designed to target the second exon of *OsIRT1* and *OsIRT2* genes. These guide RNAs, which were driven by the OsU6a promoter, were respectively cloned into the pMH-SA binary vector carrying Cas9 and digested with the restriction enzymes *Asc*I and *Spe*I. The resulting recombinant plasmids were further introduced into wild type genome via Agrobacterium-mediated gene transformation system using *Agrobacterium tumefaciens* strain EHA105. Positive transgenic plants were selected on half strength MS medium containing 50 μg/ml hygromycin, and homozygous mutants were confirmed by sequencing analysis. *OsIRT1* and *OsIRT2* were cloned downstream of the CaMV35 promoter in the pOCA30 binary vector and introduced in the Arabidopsis *irt1-3* mutant plant to generate the complementation lines *Atirt1-3/OsIRT1-OE* and *Atirt1-3/OsIRT2-OE*.

4.3. Fe content measurement

Seeds were collected from paddy fields and subjected to Fe content analysis. One-month-old seedlings grown in different hydroponic Fe solutions were used for Fe measurement. Leaves were collected and oven-dried at 65 °C for one week. Each sample was ground into powder, and approximately 500 mg dry weight was digested with 10 mL of 11 M HNO_3 and 2 mL of 12 M $HClO_4$ for 2 h at 185 °C. Samples were cooled for about 30 min, then 3 mL of 1:4 HCl was added and the final volume was adjusted to 50 mL with double-distilled water. Fe concentration was measured using inductively coupled plasma mass spectrometry (ICP-MS).

4.4. Reverse transcription and gene expression analysis

Total RNA from roots was reverse transcribed using the PrimeScript™ RT reagent Kit with gDNA Eraser according to the reverse transcription protocol (Takara, Dalian, China). Quantitative real-time PCR (qRT-PCR) was then performed using an AceQ Universal SYBR qPCR Master Mix (Vazyme, China) on a Light-Cycler 480 real-time PCR machine (Roche, Switzerland), according to the manufacturer's instructions. All PCR amplifications were performed in three biological replicates with *OsACTIN1* as an internal control. The qRT-PCR primers are listed in Table S1.

4.5. Transient expression assays

The 1k bp promoter regions from the translation start site of *OsIRT1* and *OsIRT2* were amplified and cloned into the binary vector pOCA28 harboring the nuclear localization signal of GFP (*p28-nGFP*) to generate *ProOsIRT1:nGFP* and *ProOsIRT2:nGFP* reporters. MYC-tagged OsPRI1 (MYC-OsPRI1) and mCherry-tagged OsPRI2 (mCherry-OsPRI2) were

cloned downstream of the CaMV35S promoter in the pOCA30 vector, respectively, and used as effectors. *Pro35S:MYC* and *Pro35S:mCherry* were used as negative effector controls. Cells were transformed in EHA105 strains and resuspended in infiltration buffer (10 mM $MgCl_2$, 10 mM MES, pH 5.6) at a final OD600 of 1.0. Acetosyringone was added and the solution was incubated at room temperature for 2 h without shaking. For co-infiltration, agrobacterium strains carrying different effector and reporter constructs were mixed and infiltrated into 3-week-old *Nicotiana benthamiana* leaves. The plants were incubated in dark for 48 h before fluorescence observation and RNA extraction. The transcript abundance of *GFP* was normalized to *NPTII*. Primer sequences are shown in Table S2.

4.6. Electrophoretic mobility shift assay (EMSA)

The full-length *OsPRI1* and *OsPRI2* were cloned into the pGEX vector, and the resulting plasmids were introduced into *Escherichia coli* BL21 (DE3) strains for protein expression. Cultures were incubated with 0.5 M isopropyl β-D-1-thiogalactopyranoside (IPTG) at 16 °C for 16 h, and proteins were extracted and purified using the GST-tag Protein Purification Kit (Beyotime, Shanghai, China) following the manufacturer's protocol. EMSA was performed with *OsIRT1* and *OsIRT2* promoter probes using the Chemiluminescent EMSA Kit (Beyotime) according to the manufacturer's instructions. Briefly, two complementary single-stranded DNA primers were synthesized with a biotin label at the 5′ end. The two primers were mixed and annealed to form the biotin probe. Biotin-unlabeled fragments of the same sequences or mutated sequences were used as competitors. The probe sequences are shown in Table S3.

4.7. Yeast-one-hybrid (Y1H) assay

Y1H assay was performed according to the user manual of the MatchMaker One-Hybrid System (Clontech, CA, USA). First, the coding sequences of OsPRI1 and OsPRI2 were fused to the yeast GAL4 activation domain (GAL4 AD) of pGADT7-Rec to generate the prey vectors. Next, the promoter sequences of *OsIRT1* and *OsIRT2* were inserted into the pAbAi vector upstream of the AUR1-C gene to generate the bait vectors. Each bait vector was linearized with BstbI (ThermoFisher Scientific, USA) and then transformed into the genome of *Saccharomyces cerevisiae* Y1H Gold. The cultures were grown on synthetic dextrose agar medium lacking uracil (SD/-Ura) at 30 °C for 3 days. Then, the prey vectors were co-expressed with the bait vectors harboring Y1H according to the MatchMaker One-Hybrid system user manual. One positive clone from each combination bait/prey was suspended in 0.9 % NaCl and the OD600 was adjusted to 1. The solution was then diluted to 1/10, 1/100, and 1/1000, and the cells were cultured on SD/-Leu ± Aureobasidin A (AbA: 300 ng/ml) agar plates to examine protein-DNA interactions. Prey proteins that specifically interact with the bait sequence activated the AbA resistance. All primers used are listed in Table S4.

4.8. Statistical analysis

All data were presented as means ± SD of three biological replicates. Statistical analyses were performed using the SPSS23.0 (SPSS, IBM, USA) software running one-way ANOVA according to Tukey's multiple comparison test, taking $P < 0.05$ as statistically significant.

Author contributions

Deka Reine Judesse Soviguidi1, Huaqian Ping1, 2, Bangzhen Pan1, Rihua Lei1, Gang Liang 1,*G.L. conceived the project. D.R.J.S., H.P., B. P., and R.L. performed experiments. D.R.J.S., H.P., and G.L. analyzed the data. D.R.J.S and G.L. wrote the manuscript. All authors proofread and approved the manuscript.

Data availability statement

All relevant data can be found within the paper and its supporting materials.

Funding

This work was supported by the National Natural Science Foundation of China (32370276), the Yunnan Province Postdoctoral Program (to Deka Reine Judesse Soviguidi), the Yunnan Fundamental Research Projects (202301AV070006, 202305AS350010, 202301AT070279, and 202401AT070229), and the Youth Talent Support Program of Yunnan Province (YNWR-QNBJ-2020-172).

Declaration of competing interest

The authors declare no conflicts of interest.

Acknowledgements

We thank the Institutional Center for Shared Technologies and Facilities of Xishuangbanna Tropical Botanical Garden, CAS for assistance in the determination of metal contents. We thank the Crops Conservation and Breeding Base of XTBG for rice planting.

Appendix A. Supplementary data

Supplementary data to this article can be found online at https://doi.org/10.1016/j.plaphy.2025.110059.

Data availability

Data will be made available on request.

References

Bashir, K., Hanada, K., Shimizu, M., Seki, M., Nakanishi, H., Nishizawa, N.K., 2014. Transcriptomic analysis of rice in response to iron deficiency and excess. Rice 7, 1–15. https://doi.org/10.1186/s12284-014-0018-1.

Bughio, N., Yamaguchi, H., Nishizawa, N.K., Nakanishi, H., Mori, S., 2002. Cloning an iron-regulated metal transporter from rice. J. Exp. Bot. 53, 1677–1682. https://doi.org/10.1093/jxb/erf004.

Cheng, L., Wang, F., Shou, H., Huang, F., Zheng, L., He, F., Li, J., Zhao, F.-J., Ueno, D., Ma, J.F., 2007. Mutation in nicotianamine aminotransferase stimulated the Fe (II) acquisition system and led to iron accumulation in rice. Plant Physiol. 145, 1647–1657. https://doi.org/10.1104/pp.107.107912.

Connolly, E.L., Fett, J.P., Guerinot, M.L., 2002. Expression of the IRT1 metal transporter is controlled by metals at the levels of transcript and protein accumulation. Plant Cell 14, 1347–1357. https://doi.org/10.1105/tpc.001263.

Dubeaux, G., Neveu, J., Zelazny, E., Vert, G., 2018. Metal sensing by the IRT1 transporter-receptor orchestrates its own degradation and plant metal nutrition. Mol. Cell 69. https://doi.org/10.1016/j.molcel.2018.02.009, 953-64. e5.

Divte, P.R., Yadav, P., Pawar, A.B., Sharma, V., Anand, A., Pandey, R., Singh, B., 2021. Crop response to iron deficiency is guided by cross-talk between phytohormones and their regulation of the root system architecture. Agric. Res. (Wash. D. C.) 1–14. https://doi.org/10.1007/s40003-020-00532-w.

Eide, D., Broderius, M., Fett, J., Guerinot, M.L., 1996. A novel iron-regulated metal transporter from plants identified by functional expression in yeast. Proc. Natl. Acad. Sci. 93, 5624–5628. https://doi.org/10.1073/pnas.93.11.5624.

Gautam, C.K., Tsai, H.-H., Schmidt, W., 2021. IRONMAN tunes responses to iron deficiency in concert with environmental pH. Plant Physiol. 187, 1728–1745. https://doi.org/10.1093/plphys/kiab329.

Henriques, R., Jásik, J., Klein, M., Martinoia, E., Feller, U., Schell, J., Pais, M.S., Koncz, C., 2002. Knock-out of arabidopsis metal transporter gene IRT1 results in iron deficiency accompanied by cell differentiation defects. Plant Mol. Biol. 50, 587–597. https://doi.org/10.1023/A:1019942200164.

Huang, S., Wang, P., Yamaji, N., Ma, J.F., 2020. Plant nutrition for human nutrition: hints from rice research and future perspectives. Mol. Plant 13, 825–835. https://doi.org/10.1016/j.molp.2020.05.007.

Ishimaru, Y., Suzuki, M., Ogo, Y., Takahashi, M., Nakanishi, H., Mori, S., Nishizawa, N. K., 2008. Synthesis of nicotianamine and deoxymugineic acid is regulated by OsIRO2 in Zn excess rice plants. Soil Sci. Plant Nutr. 54, 417–423. https://doi.org/10.1111/j.1747-0765.2008.00259.x.

Ishimaru, Y., Suzuki, M., Tsukamoto, T., Suzuki, K., Nakazono, M., Kobayashi, T., Wada, Y., Watanabe, S., Matsuhashi, S., Takahashi, M., 2006. Rice plants take up

iron as an Fe3+-phytosiderophore and as Fe2+. Plant J. 45, 335–346. https://doi.org/10.1111/j.1365-313X.2005.02624.x.
Ishimaru, Y., Takahashi, R., Bashir, K., Shimo, H., Senoura, T., Sugimoto, K., Ono, K., Yano, M., Ishikawa, S., Arao, T., 2012. Characterizing the role of rice NRAMP5 in manganese, iron and cadmium transport. Sci. Rep. 2, 286. https://doi.org/10.1038/srep00286.
Kobayashi, T., Nagasaka, S., Senoura, T., Itai, R.N., Nakanishi, H., Nishizawa, N.K., 2013. Iron-binding haemerythrin RING ubiquitin ligases regulate plant iron responses and accumulation. Nat. Commun. 4, 2792. https://doi.org/10.1038/ncomms3792.
Korshunova, Y.O., Eide, D., Gregg Clark, W., Lou Guerinot, M., Pakrasi, H.B., 1999. The IRT1 protein from Arabidopsis thaliana is a metal transporter with a broad substrate range. Plant Mol. Biol. 40, 37–44. https://doi.org/10.1023/A:1026438615520.
Lee, S., An, G., 2009. Over-expression of OsIRT1 leads to increased iron and zinc accumulations in rice. Plant Cell Environ. 32, 408–416. https://doi.org/10.1111/j.1365-3040.2009.01935.x.
Li, C., Li, Y., Xu, P., Liang, G., 2022. OsIRO3 Negatively Regulates Fe Homeostasis by Repressing the Expression of OsIRO2. Plant J. 111, 966–978. https://doi.org/10.1111/tpj.15864.
Li, X., Zhang, H., Ai, Q., Liang, G., Yu, D., 2016. Two bHLH transcription factors, bHLH34 and bHLH104, regulate iron homeostasis in Arabidopsis thaliana. Plant Physiol. 170, 2478–2493. https://doi.org/10.1104/pp.15.01827.
Li, C., Zhao, J., Ping, H., Li, Y., Lei, R., Pan, B., Liang, G., 2025. OsbHLH062 negatively regulates Fe homeostasis by enhancing OsHRZ1 targeting OsPRIs for degradation. New Phytol. https://doi.org/10.1111/nph.70207.
Liang, G., 2022. Iron uptake, signaling, and sensing in plants. Plant Communications. https://doi.org/10.1016/j.xplc.2022.100349.
Liang, G., Zhang, H., Li, X., Ai, Q., Yu, D., 2017. bHLH transcription factor bHLH115 regulates iron homeostasis in Arabidopsis thaliana. J. Exp. Bot. 68, 1743–1755. https://doi.org/10.1093/jxb/erx043.
Liang, G., Zhang, H., Li, Y., Pu, M., Yang, Y., Li, C., Lu, C., Xu, P., Yu, D., 2020. Oryza sativa FER-LIKE FE DEFICIENCY-INDUCED TRANSCRIPTION FACTOR (OsFIT/OsbHLH156) interacts with OsIRO2 to regulate iron homeostasis. J. Integr. Plant Biol. 62, 668–689. https://doi.org/10.1111/jipb.12933.
Liang, G., Zhang, H., Lou, D., Yu, D., 2016. Selection of highly efficient sgRNAs for CRISPR/Cas9-based plant genome editing. Sci. Rep. 6, 21451. https://doi.org/10.1038/srep21451.
Liu, Y., Ji, X., Nie, X., Qu, M., Zheng, L., Tan, Z., Zhao, H., Huo, L., Liu, S., Zhang, B., 2015. Arabidopsis atb HLH 112 regulates the expression of genes involved in abiotic stress tolerance by binding to their e-box and GCG-box motifs. New Phytol. 207, 692–709. https://doi.org/10.1111/nph.13387.
Long, L., Persson, D.P., Duan, F., Jørgensen, K., Yuan, L., Schjoerring, J.K., Pedas, P.R., 2018. The iron-regulated transporter 1 plays an essential role in uptake, translocation and grain-loading of manganese, but not iron, in barley. New Phytol. 217, 1640–1653. https://doi.org/10.1111/nph.14930.
Mahawar, L., Ramasamy, K.P., Pandey, A., Prasad, S.M., 2023. Iron deficiency in plants: an update on homeostasis and its regulation by nitric oxide and phytohormones. Plant Growth Regul. 100, 283–299. https://doi.org/10.1007/s10725-022-00853-6.
Ning, X., Lin, M., Huang, G., Mao, J., Gao, Z., Wang, X., 2023. Research progress on iron absorption, transport, and molecular regulation strategy in plants. Front. Plant Sci. 14, 1190768. https://doi.org/10.3389/fpls.2023.1190768.
Pasricha, S.-R., Tye-Din, J., Muckenthaler, M.U., Swinkels, D.W., 2021. Iron deficiency. Lancet 397, 233–248. https://doi.org/10.1016/S0140-6736(20)32594-0.
Pedas, P., Ytting, C.K., Fuglsang, A.T., Jahn, T.P., Schjoerring, J.K., Husted, S., 2008. Manganese efficiency in barley: identification and characterization of the metal ion transporter HvIRT1. Plant Physiol. 148, 455–466. https://doi.org/10.1104/pp.108.118851.
Peng, F., Li, C., Lu, C., Li, Y., Xu, P., Liang, G., 2022. IRONMAN peptide interacts with OsHRZ1 and OsHRZ2 to maintain Fe homeostasis in rice. J. Exp. Bot. 73, 6463–6474.
Pradhan, S., Pandit, E., Pawar, S., Pradhan, A., Behera, L., Das, S., Pathak, H., 2020. Genetic regulation of homeostasis, uptake, bio-fortification and efficiency enhancement of iron in rice. Environ. Exp. Bot. 177, 104066. https://doi.org/10.1016/j.envexpbot.2020.104066.
Rai, S., Singh, P.K., Mankotia, S., Swain, J., Satbhai, S.B., 2021. Iron homeostasis in plants and its crosstalk with copper, zinc, and manganese. Plant Stress 1, 100008. https://doi.org/10.1016/j.stress.2021.100008.
Robinson, N.J., Procter, C.M., Connolly, E.L., Guerinot, M.L., 1999. A ferric-chelate reductase for iron uptake from soils. Nature 397, 694–697. https://doi.org/10.1038/17800.
Rogers, E.E., Eide, D.J., Guerinot, M.L., 2000. Altered selectivity in an arabidopsis metal transporter. Proc. Natl. Acad. Sci. 97, 12356–12360. https://doi.org/10.1073/pnas.210214197.
Soviguidi, D.R.J., Duan, Z., Pan, B., Lei, R., Liang, G., 2025. Function, structure, and regulation of iron regulated transporter 1. Plant Physiol. Biochem. 219, 109457. https://doi.org/10.1016/j.plaphy.2024.109457.
Takagi, S.-i., 1976. Naturally occurring iron-chelating compounds in oat-and rice-root washings: I. Activity measurement and preliminary characterization. Soil Sci. Plant Nutr. 22, 423–433. https://doi.org/10.1080/00380768.1976.10433004.
Takagi, S.i., Nomoto, K., Takemoto, T., 1984. Physiological aspect of mugineic acid, a possible phytosiderophore of graminaceous plants. J. Plant Nutr. 7, 469–477. https://doi.org/10.1080/01904168409363213.
Varotto, C., Maiwald, D., Pesaresi, P., Jahns, P., Salamini, F., Leister, D., 2002. The metal ion transporter IRT1 is necessary for iron homeostasis and efficient photosynthesis in Arabidopsis thaliana. Plant J. 31, 589–599. https://doi.org/10.1046/j.1365-313X.2002.01381.x.
Vert, G., Barberon, M., Zelazny, E., Séguéla, M., Briat, J.-F., Curie, C., 2009. Arabidopsis IRT2 cooperates with the high-affinity iron uptake system to maintain iron homeostasis in root epidermal cells. Planta 229, 1171–1179. https://doi.org/10.1007/s00425-009-0904-8.
Vert, G., Briat, J.F., Curie, C., 2001. Arabidopsis IRT2 gene encodes a root-periphery iron transporter. Plant J. 26, 181–189. https://doi.org/10.1046/j.1365-313x.2001.01018.x.
Vert, G., Grotz, N., Dédaldéchamp, F., Gaymard, F., Guerinot, M.L., Briat, J.-F., Curie, C., 2002. IRT1, an arabidopsis transporter essential for iron uptake from the soil and for plant growth. Plant Cell 14, 1223–1233. https://doi.org/10.1093/plcell/koaa033.
Wairich, A., Oliveira, B.H.N.d., Arend, E.B., Duarte, G.L., Ponte, L.R., Sperotto, R.A., Ricachenevsky, F.K., Fett, J.P., 2019. The combined strategy for iron uptake is not exclusive to domesticated rice. Sci. Rep. 9, 17. https://doi.org/10.1038/s41598-019-52502-0, 2019), 16144.
Wang, H.-Y., Klatte, M., Jakoby, M., Bäumlein, H., Weisshaar, B., Bauer, P., 2007. Iron deficiency-mediated stress regulation of four subgroup Ib BHLH genes in Arabidopsis thaliana. Planta 226, 897–908. https://doi.org/10.1007/s00425-007-0535-x.
Wang, S., Li, L., Ying, Y., Wang, J., Shao, J.F., Yamaji, N., Whelan, J., Ma, J.F., Shou, H., 2020. A transcription factor OsbHLH156 regulates strategy II iron acquisition through localising IRO2 to the nucleus in rice. New Phytol. 225, 1247–1260. https://doi.org/10.1111/nph.16232.
Wang, W., Ye, J., Xu, H., Liu, X., Fu, Y., Zhang, H., Rouached, H., Whelan, J., Shen, Z., Zheng, L., 2022. OsbHLH061 links TOPLESS/TOPLESS-RELATED repressor proteins with POSITIVE REGULATOR OF IRON HOMEOSTASIS 1 to maintain iron homeostasis in rice. New Phytol. 234, 1753–1769. https://doi.org/10.1111/nph.18096.
Yuan, Y., Wu, H., Wang, N., Li, J., Zhao, W., Du, J., Wang, D., Ling, H.-Q., 2008. FIT interacts with AtbHLH38 and AtbHLH39 in regulating iron uptake gene expression for iron homeostasis in arabidopsis. Cell Res. 18, 385–397. https://doi.org/10.1038/cr.2008.26.
Zhang, H., Li, Y., Pu, M., Xu, P., Liang, G., Yu, D., 2020. Oryza sativa POSITIVE REGULATOR OF IRON DEFICIENCY RESPONSE 2 (OsPRI2) and OsPRI3 are involved in the maintenance of Fe homeostasis. Plant Cell Environ. 43, 261–274. https://doi.org/10.1111/pce.13655.
Zhang, H., Li, Y., Yao, X., Liang, G., Yu, D., 2017. Positive regulator of iron homeostasis1, OsPRI1, facilitates iron homeostasis. Plant Physiol. 175, 543–554. https://doi.org/10.1104/pp.17.00794.